www.amlett.org, www.amlett.com, DOI: 10.5185/amlett.2012.7391 Published online by the VBRI press in 2013

Study of optical and ferroelectric behavior of ZnO nanostructures

Prakash Chand, Anurag Gaur*, Ashavani Kumar

Department of Physics, National Institute of Technology, Kurukshetra 136119, India

*Corresponding author. Tel: (+91) 1744-233549; Fax: (+91) 1744-238050; E-mail: anuragdph@gmail.com

Received: 05 July 2012, Revised: 08 August 2012 and Accepted: 09 August 2012

ABSTRACT

In the present work, we have synthesized ZnO nanostructures by sol-gel method in air at different selected sintering temperatures ranging from room temperature to 400 ^{0}C and studied their structural, optical and ferroelectric properties. The synthesized samples are characterized by X-ray diffractrometer for structural properties and the optical properties are measured through UV-Visible spectrophotometer and Photoluminescence. The X-ray diffraction pattern indicates the pure phase formation of ZnO. Furthermore, photoluminescence spectra also confirm the formation of wurtzite structure of ZnO. X-ray diffraction (XRD) and Transmission Electron Microscope (TEM) studies show that the particle size of ZnO nanostructures increases with increasing the sintering temperature. The optical band gaps calculated through UV spectroscopy are found to be decreasing from 4.47 to 3.73 eV for samples sintered at room temperature to 400 ^{0}C, respectively. Moreover, a weak ferroelectricity has been observed in ZnO nanostructures at room temperature through Polarization vs Electric field (*P-E)* loops.

Keywords: ZnO nanostructures; optical and ferroelectric properties.

Prakash Chand is working as an Assistant Professor in Department of Physics, National Institute of Technology, Kurukshetra. He did his M.Sc. in Physics from Kurukshetra University Kurukshetra and pursuing Ph.D at National Institute of Technology, Kurukshetra. His main researches interests include transition metal oxides based nanostructures.

Anurag Gaur received his Ph.D. degree from Indian Institute of Technology Roorkee in 2007. He is presently working as an Assistant Professor in Department of Physics, National Institute of Technology, Kurukshetra. He is leading one D.S.T., Govt of India funded research project on Multiferroics. His other fields of interests are Functional Nanostructured Oxide materials such as Double Perovskite based Magnetoresistive materials, Ferrites and Diluted Magnetic semiconductors. He has published more than twenty five research papers in leading journals and is the reviewer of many International journals.

Ashvani Kumar is working as Associate Professor in the Department of Physics, National Institute of Technology, Kurukshetra. He did his Ph.D. in Physics from Aligarh Muslim University (AMU), Aligarh, India. He is also leading one D.S.T., Govt of India funded research project on high energy physics. He has published more than fifty research papers in international journals and reviewer of many International journals. His main research interests include radiation shielding and hadrontherapy using high Z particles as well as synthesis and characterization of nanomaterials for their applications in sensing devices like night vision cameras etc.

Introduction

Over the past few years, metal oxide semiconductors play important roles in many areas of science and technology and have attracted great interest due to their significant potential application. Among metal oxides, ZnO has attracted a great interest due to their importance in both scientific research and potential technological applications. ZnO is emerging as a material of interest for a variety of electronic applications. It can be used in a large number of areas, and unlike many of the materials with which it competes, zinc oxide is inexpensive, relatively abundant, easy to prepare and non-toxic. ZnO is a II-VI semiconductor also known as zincite with a direct band gap of 3.37eV with excitonic energy of 60 meV that is significantly larger than the thermal energy at room temperature which corresponds to 26 meV. It is thermally and chemically stable and presents interesting properties **[1-6]**. It crystallizes in a hexagonal wurtzite structure with lattice parameters; (a=3.24Å, c=5.21Å). ZnO receiving a lot of attention because of its wide direct band gap, strong excitonic binding energy and potentials applications in transparent conducting electrodes, light emitting diodes (LED), solar cells piezoelectric devices, chemical sensors, catalysis, actuation, optoelectronic devices and drug delivery **[7-9]**. Nano sized zinc oxide due to the large band gap and high exciton binding energy shows various useful properties and gives large and diverse range of growth of

different type of morphologies such as nanorods, nanosheets, nanocombs, nanobelts, nanowires and nanorings, which may be used in various applications **[10-13]**. ZnO is also an ideal material for studying the transport processes in one dimensionally confined object, which are important for the development of high performance nano devices, including sensors, ultra violet/blue emission devices, field emission devices **[14]**. In the recent years much attention has been paid to the synthesis, characterization and applications of these nanoparticles due to their excellent unique size dependent properties **[15]**. Among the various morphologies of ZnO nanostructures, ZnO have potential applications in short-wave light-emitting photonic devices due to their strong ultraviolet (UV) emission at room temperature **[16-19]**. There are various synthesis route for the preparation of ultrafine oxide nanoparticles such as sol- gel, hydrothermal, flame combustion, emulsion precipitation, fungus mediated biosynthesis, microwave irradiation, solid–vapour deposition, solid state reaction, conventional precipitation, and wet chemical methods **[20-32]**. The sol–gel process is one of the best methods for synthesizing high purity advanced materials with control in the nanostructure and surface properties **[20]**. Furthermore, recently few groups reported the ferroelectricity in doped ZnO at room temperature **[33-34]**.

Therefore, in the present work, we synthesized ZnO nanostructures by sol-gel method and studied the structural, optical and ferroelectric properties. It is observed that the particle size of ZnO nanostructures increases while optical band gap decreases as we increase the sintering temperature. Moreover, a weak ferroelectric nature has been observed in these ZnO nanostructures at room temperature, which adds an additional dimension to its applications and appears a novel result.

Experimental

Materials

For the preparation of ZnO nanostructures, the materials used were zinc acetate dehydrate [Zn $(CH_3COO)_2.2H_2O$, 99 %, Merck, Mumbai, India), Potassium hydroxide (KOH, 98%, Merck, Mumbai, India), absolute ethanol (CH_3CH_2OH, 99.9%, Changshu Yangyuan Chemical, China) and double distilled water (Jairavik, New Delhi, India). All Chemicals used in the presents work were of analytical grade and were used without further purifications.

Synthesis of ZnO nanostructures

To prepare the ZnO nanostructures, the high purity zinc acetate dehydrate [Zn $(CH_3COO)_2.2H_2O$], was dissolved in 50 ml of double distilled water under vigorous stirring and a 6M Potassium hydroxide (KOH) solution was then added drop wise with constant stirring to give a milky white $Zn(OH)_2$ gel . This $Zn(OH)_2$ gel was filtered and washed several times with distilled water and ethanol to remove the impurities ions and then centrifuged and dried at room temperature. The as synthesized powders are sintered at different temperature from room temperature to 400 ^{0}C, to vary the particle size.

Characterization

The synthesized samples were characterized by X-ray diffractometer (XRD; Rigaku Japan) with Cu-Kα radiation source (λ=1.54059 Å) for structural and phase analysis. Data is collected with a counting rate of 2^0 per minutes in the range of 2θ from 20 to 80^0. The morphology and the structural characterization were conducted by transmission electron microscope (TEM; Hitachi model 7500, Ltd., Tokyo, Japan). Diluted nanoparticles were suspended in absolute ethanol and put on a carbon coated copper grid, and were allowed to dry in air for conducting TEM images. The optical properties of the nanostructures were studied by UV-visible spectrophotometer (Camspec M550 Double Beam Scanning) and Photoluminescence (PL; Varian, Cary Eclipe Fluorescence spectrophotometer) with excitation wavelength 250 nm.

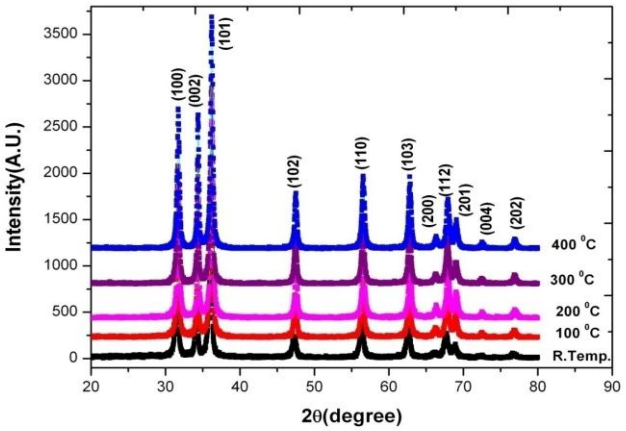

Fig. 1. Room temperature XRD patterns of ZnO nanostructures sintered at different temperatures.

Results and discussion

X-Ray diffraction studies

The XRD patterns of ZnO particles sintered at different temperatures are shown in **Fig. 1**. The XRD pattern indicates the pure wurtzite phase formation of ZnO without any impurity phase for all the samples sintered at different temperatures (room temperature to 400 ^{0}C). The corresponding X-ray diffraction peak for (100), (002) and (101) planes confirm the formation of wurtzite structure of ZnO. From **Fig. 1**, it can be observed that the peak positions are identical for all the samples sintered at room temperature to 400 ^{0}C, which indicate that there is no significant change in the lattice parameters. With increasing the sintering temperature, the intensity of the major diffraction peaks increases indicating that the crystallization of ZnO nanostructure improves at higher sintering temperature. However, the observed line broadening of the diffraction peaks is an indication that the synthesized materials are in nanometer range which is further confirmed by TEM analysis. The average crystallite size (t) of ZnO nanoparticles is calculated by using Scherrer formula: $D \sim K \lambda / \beta \cos\theta_B$, where k~0.89 is the shape factor, λ is wavelength of CuKα (1.54059 ˚A) radiation, β=B-b, B is the full width at half maximum (FWHM), b represents the instruments broadening and θ_B is the angle of Bragg diffraction. The particle size, calculated by Debye Scherrer

formula using XRD data, increases from 13 to 31 nm for the samples sintered at room temperature to 400 ^{0}C, respectively.

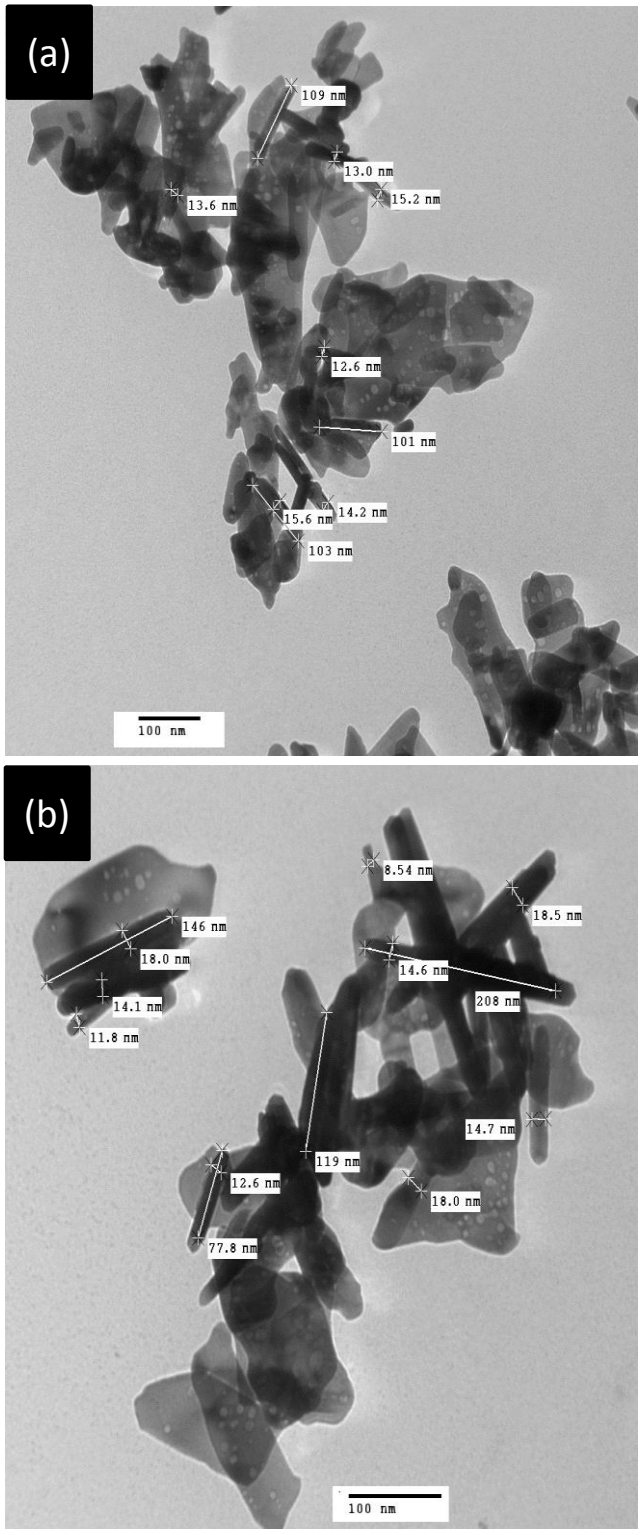

Fig. 2. Transmission Electron Microscopy (TEM) images of zinc oxide nanostructures sintered at (a) 100 ^{0}C and (b) 400 ^{0}C.

TEM studies

The structural morphology and size of the as synthesized ZnO nanostructures were investigated using TEM. The TEM images of ZnO nanostructures were taken with a resolution of 2Å and are shown in **Fig. 2**. **Fig. 2** shows the TEM images of ZnO nanostructures sintered at 100 and 400 ^{0}C, respectively. It is seen that all particles crystallized in a rod shape with an average diameter and length of 12 and 104 nm for samples sintered at 100 ^{0}C and 15 and 138 nm for samples sintered at 400 ^{0}C, respectively. It is clear from TEM images that the diameter of the nanorods grows with increase in the sintering temperature. Therefore, the particle size is greatly dependent on the sintering temperature. As the sintering temperature increases, the size also increases, due to congregation effect. Evidently, the sintering temperature promotes enlargement of grain boundaries and consequently particle size increases. This also supports the XRD analysis that average diameter of these nanorods increases with increasing the sintering temperature.

Photoluminescence studies

Photoluminescence is a powerful tool for providing essential information about the physical properties of materials at molecular levels, including shallow and deep level defects and band gap state for energy level **[35]**. The effect of sintering temperature on the PL properties of ZnO nanostructures was investigated. The PL spectra obtained at room temperature for ZnO nanostructures sintered at different selected temperatures from room temperature to 400 ^{0}C and are shown in **Fig. 3**. The PL spectra in all samples exhibit one prominent emission peak at 422 nm in the UV position and a broad blue band are centered at 486 nm. The PL signal at 422 nm is a typical near band edge UV emission of ZnO which indicates a direct recombination of excitons through an exciton-exciton collision process **[36]**. The luminescence blue bands at 486 nm are due to transition vacancy of oxygen and interstitial oxygen. The appearance of sharp and strong UV emission and a broad blue band emission in the PL spectra indicates that the ZnO nanorods have good crystallization quality with excellent optical properties.

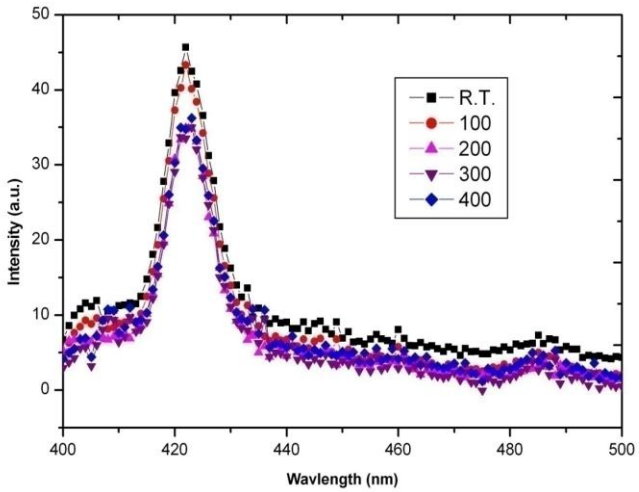

Fig. 3. Room temperature photoluminescence (PL) spectrum of ZnO nanostructures sintered at different temperatures.

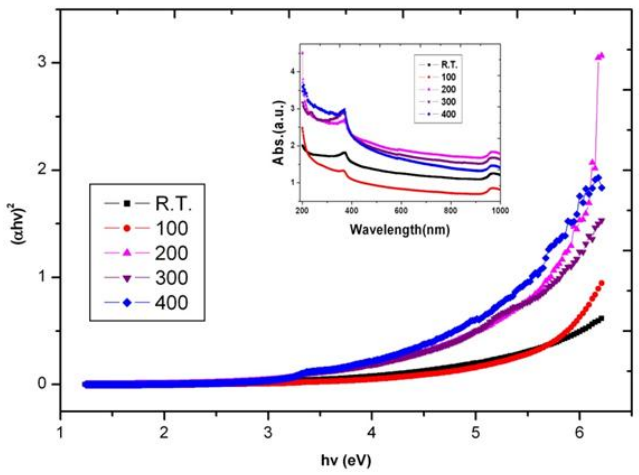

Fig. 4 $(\alpha h\nu)^2$ versus Photon energy (hv) plot for ZnO nanostructures sintered at different temperatures. The inset of Fig. 4 shows absorbance versus wavelength plots**.**

UV-visible studies

The optical properties of ZnO nanostructures are studied by analyzing the UV-Vis spectra as shown in **Fig. 4**. The inset of **Fig. 4** shows absorbance versus wavelength plots for ZnO nanostructures sintered at different temperatures. For the UV–vis absorption measurement, the as-prepared ZnO sample is ultrasonically dispersed in absolute ethanol before examination, using absolute ethanol as the reference. It is clearly seen that the absorbance decreases with an increase in wavelength, and a sharp decrease in absorbance near the band edge (367 nm) indicating the crystallinity of the samples. The optical band gap of ZnO nanostructures are estimated using the transition rate equation for direct band gap semiconductor. The absorption coefficient for direct transition is given by the equation: $\alpha(h\nu) = A(h\nu - E_g)^n$ where hv= photon energy, α= absorption coefficient ($\alpha=4\pi k/\lambda$; k is the absorption index or absorbance, λ is the wavelength in nm), Eg is the band gap energy. A= constant, n= ½ for the allowed direct band. The exponent 'n' depends on the type of transition and it may have values 1/2, 2, 3/2 and 3 corresponding to the allowed direct, allowed indirect, forbidden direct and forbidden indirect transitions respectively **[37-38]**. The direct band gap energies were calculated by plotting Tauc's graphs between $(\alpha h\nu)^2$ versus photon energy (hv) for ZnO nanostructures sintered at different selected temperatures from room temperature, 100, 200, 300 and 400 ^{0}C respectively. The intercept of the tangent to the plot on the X-axis gives the direct band gap of ZnO nanostructures. The optical band gaps calculated through UV spectroscopy are found to 4.47, 4.35, 4.19, 3.96 and 3.73 eV for samples sintered at room temperature, 100, 200, 300 and 400 ^{0}C, respectively. The band gaps calculated through UV-visible spectroscopy are also shown in **Table 1**. It can be observed that the band gap decreases with increasing sintering temperatures. The reduction of band gap with sintering temperature is due to the decrease of gap between conduction band edge and valance band edge of the zinc oxide nanostructures. As temperature increases, the band gap energy decreases because the crystal lattice expands and the interatomic bonds are weakened. Weaker bonds means less energy is needed to break a bond and get an electron in the conduction band. The observed small band gap may also be attributed to the energy levels in the intrinsic gap due to the defects such as oxygen vacancies and Zn ions at the interstitial sites. These results showed a strong correlation between sintering temperature and the properties of ZnO nanostructures.

Table 1. Variations of E_{max}, E_c, P_s, P_r and energy band gap of ZnO nanostructures sintered at different temperatures.

Sintering temperature (^{0}C)	E_{max} (kV/cm)	E_c (kV/cm)	P_r (μC/cm^2)	P_s (μC/cm^2)	Band gap (eV)
Room Temperature	000.545	000.062	000.117	000.943	4.47
100	000.522	000.237	003.161	000.117	4.35
200	000.525	000.187	009.540	000.515	4.19
300	000.553	000.087	012.606	000.389	3.96
400	004.849	001.186	000.259	001.473	3.73

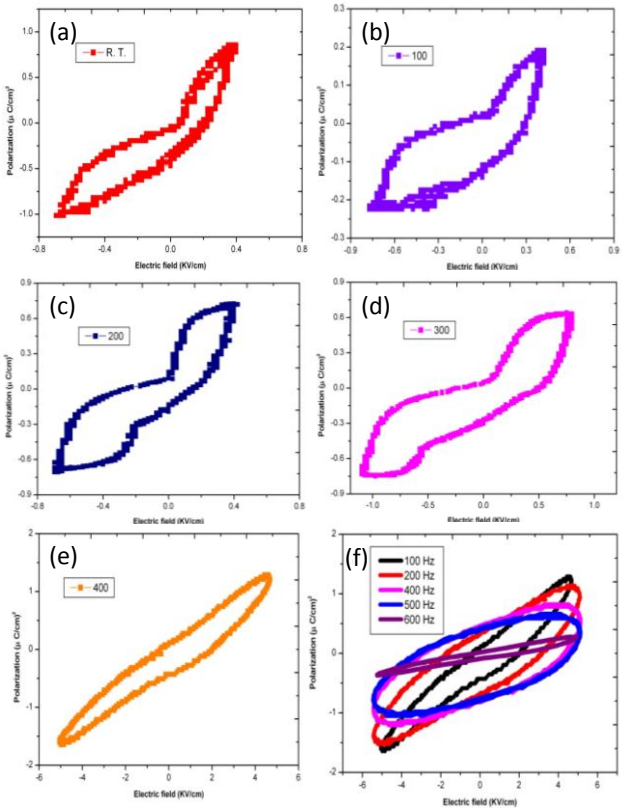

Fig. 5. (a-e) P-E hysteresis loops of ZnO nanostructures sintered at different temperatures at fixed f=100 Hz and (f) shows P-E hysteresis loops of ZnO nanostructures sintered at 400 ^{0}C with varying frequency.

Ferroelectric studies

Fig. 5 (a-f) shows the ferroelectric hysteresis loop of ZnO sintered at different selected temperature ranging from room temperature to 400 ^{0}C, obtained under a maximum applied electric field of 2 kVcm^{-1} for room temperature & 100 ^{0}C and 6 kVcm^{-1} for 200 ^{0}C, 300 ^{0}C and 400 ^{0}C. The loop indicates weak ferroelectricity for the sample sintered at different selected temperature that might be due to the fact of relatively high-leakage current. The remnant polarization P_r (μC/cm^2) and coercive field E_c (kV/cm), Emax (kV/cm) and P_s (μC/cm^2) of ZnO nanostructures

sintered at different selected temperature are shown in **Table 1**. The value of remnant polarization (P_r) increases from 000.117 to 012.606 μC/cm^2 for the samples sintered from room temperature to 300 ^{0}C and then decreases.

Furthermore, we have also studies the Polarization vs Electric field (*P-E)* loops at different frequencies (from 100 to 600 Hz) of ZnO nanostructures and are shown in **Fig.5 (f)**. The loop again indicates weak ferroelectricity. Such relatively low-quality hysteresis might be due to the fact of relatively high-leakage current. It is clear from the **Fig. 5 (f)** that the saturation found to be decrease with increasing frequencies. That is as the applied frequency increased, the P-E loop gets unsaturated. This is because as the frequency increases, the conducting nature of the sample increases and hence loop gets unsaturated at higher frequencies. The hysteresis area of ZnO nanostructures decreases with increasing frequency because at high frequency, the switching domains are delayed in flipping domain direction following applied electric field direction. When apply higher frequency, the switching domains are more delayed. This causes a decrease of hysteresis area when frequency increases.

Conclusion

In this work, we have successfully synthesized ZnO nanoparticles by sol-gel method and studied the effects of sintering temperatures on the structural, optical and ferroelectric properties. The XRD results indicate that all samples sintered at different temperature (room temperature to 400 ^{0}C) have the pure wurtzite ZnO phase without any impurity. Furthermore, photoluminescence spectroscopy also confirms the formation of wurtzite structure of ZnO. The optical band gaps calculated through UV spectroscopy are found to be decreasing from 4.47 to 3.73 eV for samples sintered from room temperature to 400 ^{0}C, respectively. Interestingly, the observation of weak ferroelectric nature in these ZnO nanostructures at room temperature adds an additional dimension to its applications.

Acknowledgements

The authors would like to thank the following institutions for providing technical support: SAIF CIL, Punjab University Chandigarh for TEM studies, CSIO, for PL analysis. The authors are also grateful to Director, NIT Kurukshetra for providing the facilities in Physics Department.

Reference

1. Gao, Z.; Gu, Y.; Zhang, Y. *Journal of Nanomaterials* **2010**, **DOI:**10.1155/2010/462032.
2. Singh, D. P. *Science of Advanced Materials*, **2010**, 2, 245.
3. Mohanta, S. K.; Kim, D. C.; Kong, B. H.; Cho, H. K.; Liu, W. ; Tripathy, S. *Science of Advanced Materials*, **2010**, 2, 64.
4. Irimpan, L.; Nampoori, V. P. N.; Radhakrishnan, P. *Science of Advanced Materials*, **2010,** 2, 578.
5. Tiwari**,** A.; Mishra, A.K.; Kobayashi, H.; Turner, Anthony PF, *Intelligent Nanomaterials*, **2012**, Wiley-Scrivener Publishing LLC, USA, ISBN 978-04-709387-99.
6. Okazaki, K.; Kubo, K.; Shimogaki, T.; Nakamura, D.; Higashihata, M.; Okada, T.; *Adv. Mat. Lett*. **2011**, 2(5), 354.
7. Shakti, N.; Gupta, P. S. *Applied Physics Research*, **2010,** 2**,** 19.
8. Law, M.; Greene, L.E.; Johnson, J. C.; Saykally, R.; Yang, P.D. *Nature Materials* **2005,** 4, 455. `
9. Tian, Z.R.; Voigt, J. A.; Liu, J.; Mckenzie, B.; Mc Dermott, M. J.; Rodriguez, M. A.; Kingishi, H.; Xu, H. *Nat. Mater*. **2003**, *2*, 821. **DOI:** 10.1038/nmat1014
10. Feng, X.; Ke, Y.; Guodong, L.; Qiong, L.; Ziqiang, Z. *Nanotech.* **2006**, *17*, 2855. **DOI:**10.1088/0957-4484/17/12/005
11. Wei, Q.; Meng, G.; An, X.; Hao Y.; Zang, L. *Nanotech.*, **2005**, *16*, 2561. **DOI:**10.1088/0957-4484/16/11/016
12. Kim, C.; Chun, M. J.; Kim, D.E. *Nanotech.*, **2005**, *16*, 2104.
13. Reddy, R. Subba; Sreedhar, A.; Reddy, A. Sivasankar; Uthanna, S., *Adv. Mat. Lett*. **2012**, 3(3), 239.
14. Palani, I.A.; Nakamura, D. K.; Okazaki, T.; Shimogaki, M.; Higashihata, T. Okada,
15. *Adv. Mat. Lett*. **2012**, 3(2), 66.
16. Dutta, R. K.; Sharma, P. K.; Pandey, A. C., Adv. *Mat. Lett*. **2011**, 2(4), 268.
17. Zhu, Z. Q.; Zhou, J. G.; Liu, Z. ; Ren, Z. G. *Rare Met.* **2008**, 5, 27.
18. Cao, H.; Xu, J. Y.; Zhang, D. Z.; Chang, S. H.; Ho, S. T.; Seelig, E. W.; Liu, X.; Chang, R. P. H. *Phys. Rev. Lett.* **2000,** 84**,** 5584.
19. Huang, M. H.; Wu, Y.; Feick, H.; Tran, N.; Weber, E. ; Yang, P. *Adv. Mater.* **2001,** 13, 113.
20. Wang, Z. L. *J. Phys. Condens. Matter*, **2004,** 16**,** 829.
21. Moghaddam, A. B.; Nazari, T.; Badraghi, J.; Ka-zemzad, M. *Int. J. Electrochem. Sci*, **2009,** 4**,** 247.
22. Shokuhfar, T.; Vaezi, M. R.; Sadrnezhad, S. K.; Sho-kuhfar, A. *Int. J. Nanomanu-facturing*, **2008,** 2, 149.
23. Kim, S. J.; Park, D. W. *Appl. Chem.*, **2007,** 11**,** 377.
24. Vaezi, M. R.; Sadrnezhaad, S. *Ma-ter Design*, **2007,** 28**,** 515.
25. Ge, M. Y.; Wu, H. P.; Niu, L.; Liu, J.F., Chen, S.Y., Shen, P. Y.; Zeng, Y. W.; Wang, Y. W.; Zhang, G. Q. ; Jiang, J. Z. *J. Cryst. Growth*, **2007,** 305**,** 162.
26. Ahmed, F.; Kumar, S.; Arshi, N.; Anwar, M.S.; Prakash, R.; *Adv. Mat. Lett.* **2011**, 2(3), 183.
27. Srivastava, A.K.; Deepa, M.; Sood, K.N.; Erdem, E.; Eichel, R.A.; *Adv. Mat. Lett*. **2011**, 2(2), 142.
28. Sharma, V. K.; Najim, M.; Varma, G. D. *Adv. Mat. Lett*. **2012**, 3(2), 107.
29. Srivastava, R.; Yadav, B. C.; *Adv. Mat. Lett*. **2012**, 3(3), 197.
30. Verma, I.; Kumar, Ritesh; Verma, Nidhi, *Adv. Mat. Lett*. **2012**, 3(3), 250.
31. Kant, S.; Kumar, A. Adv. Mat. Lett. 2012, **3**(4), 350.
32. Shukla, S.K.; Tiwari, A.; Parashar, G.K.; Mishra, A.P.; Dubey , G. C. *Talanta* **2009**, 80, 565.
33. Shukla, S.K.; Deshpande, S. R.; Shukla, S.K.; Tiwari, A. *Talanta*, **2012**.99, 283. **DOI:** 10.1016/j.talanta.2012.05.052
34. Lin, Yuan-Hua; Ying, Minghao; Li, Ming; Wang, Xiaohui ; Nan, Ce-Wen *Appl.Phys.Lett.* **2007,** 90, 222110.
35. Kim, Jin Soo; Lee, Hai Joon; Seog, Hae Jin and Kim, III Won *J. Korean Phys. Soc*. **2011**, 58, 640.
36. Blasse, G.; Grabmaier, B. C. *Luminescent Materials*, Springer-verlag Berlin New York, **1994**.
37. Yang, Y.; Wang, X. H.; Sun, C. K.; Li, L. T. *Journal of Applied physics* **2009**, 9, 105.
38. Tauc, J. Amrphous and Liquid Semiconductors, Plenum Press, London, **1974**, 8.
39. Singh, J. P.; Srivastava, R. C.; Agarwal, H. M. *A. I. P. Proced*. **2010,** 137, 1276.

